Applied Physics Reviews ARTICLE pubs.aip.org/aip/are

Boundary conditions dictate frequency dependence of thermal conductivity in silicon

Cite as: Appl. Phys. Rev. **12**, 031421 (2025); doi: 10.1063/5.0254248
Submitted: 21 December 2024 · Accepted: 4 September 2025 ·
Published Online: 19 September 2025

Yizhe Liu,[1] Qinshu Li,[1] Fang Liu,[2] Xinqiang Wang,[2,3] and Bo Sun[1,4,a)]

AFFILIATIONS

[1]Tsinghua SIGS, Tsinghua University, Shenzhen 518055, China
[2]State Key Laboratory for Mesoscopic Physics and Frontiers Science Center for Nano-optoelectronics, School of Physics, Peking University, Beijing 100871, China
[3]Peking University Yangtze Delta Institute of Optoelectronics, Nantong, Jiangsu 226010, China
[4]Guangdong Provincial Key Laboratory of Thermal Management Engineering & Materials, Shenzhen 518055, China

[a)]**Author to whom correspondence should be addressed:** sun.bo@sz.tsinghua.edu.cn

ABSTRACT

Non-Fourier thermal transports have drawn significant attention for decades. Among them, the frequency-dependent thermal conductivity has been extensively explored by pump-probe techniques, such as time-domain thermoreflectance, which is employed to probe the spectra of phonon mean free paths. However, previous studies on silicon have not exhibited apparent frequency dependence despite its broad phonon distribution. Here, we report the frequency-dependent thermal transport in Al/Si with an atomically sharp interface, where the matched Debye temperatures preserve the temperature difference between low- and high-energy phonons in Si and contribute as additional non-equilibrium thermal resistance. The dependence vanishes in Al/SiO_2/Si at room temperature, since the SiO_2 interlayer facilitates phonon scattering and destroys thermal non-equilibrium. At 80 K, frequency dependence reemerges in Al/SiO_2/Si due to reduced interfacial phonon scattering, which is not sufficient to destroy the temperature difference between low- and high-energy phonons. The frequency dependence is weakened in the Al/Si sample at 500 K, originating from the enhanced phonon scattering rate in Si. Our findings highlight the significance of boundary conditions in frequency-dependent thermal conductivity.

I. INTRODUCTION

Heat transports diffusively when carrier mean free paths (MFPs) are shorter than the characteristic length of the temperature profile, as described by Fourier's law. In high-frequency electronic devices, periodic Joule heating leads to a restricted temperature profile.[1] As a result, the important temperature lengths diminish to the carrier MFPs, and non-Fourier transport appears.[2–8] Consequently, thermal conductivity (Λ) shows a dependence on heating frequency, with a marked suppression when the heat diffusion length approaches phonon MFPs.[9]

Experimental demonstrations on the frequency dependence of thermal transport have been achieved through pump-probe studies with periodic heating at several MHz on semiconductor alloys,[10] and later on graphite[11] and other two-dimensional materials.[12,13] The observed frequency-dependent Λ was initially attributed to a broad spectrum of phonon MFPs by Koh *et al.*,[10] where phonons with MFPs longer than the important temperature lengths could not be probed, thus motivating innovative experiments to measure phonon spectra.[11,12,14–16] Furthermore, Wilson *et al.* interpreted the frequency-dependent thermal transport using a two-channel model based on the phonon non-equilibrium, where weak interactions between low- and high-frequency phonons constitute additional non-equilibrium resistance,[17] dictated by the transducer/sample interface. This model successfully explained the reduction in apparent Λ (at high frequencies) and thermal conductance G (at low frequencies) in SiGe alloys[17] and transition metal dichalcogenides,[13] enriching the understanding of phonon dynamics. Additionally, a ballistic/diffusive model was proposed to explain non-Fourier transports within time-domain thermoreflectance (TDTR) and broadband frequency-domain thermoreflectance (BB-FDTR) experiments, where ballistic phonons carry less heat than Fourier's law predictions, and the reduced Λ originates from the reflection of long MFP phonons at the interface.[18] Importantly, both theories reveal the critical influence of the interface on frequency-dependent thermal transport, thus underscoring the significance of the transducer/sample boundary condition.

However, a comprehensive understanding of the observed frequency dependence remains elusive with certain puzzles. For example,

Si displays a broader spectral distribution of phonon MFPs, compared to two-dimensional materials displaying frequency-dependent Λ along the through-plane direction.[14,19] Nevertheless, previous TDTR measurements on Si at room temperature (RT) did not reveal apparent frequency dependence, regardless of the transducer/Si boundary conditions. Moreover, although previous experiments have reported that the transducer/sample interface affects the frequency dependence,[14,15,18] the underlying mechanisms is still incomplete, impeding accurate measurements of intrinsic thermal properties.

In this work, we discover a pronounced frequency-dependent thermal transport in TDTR measurements on Al/Si with an atomically sharp interface. The atomically sharp Al/Si interface, with matched phonon density of states (DOS), minimizes interfacial phonon scattering, preserving the phonon non-equilibrium in Si. In contrast, the Al/SiO_2/Si interface with a SiO_2 barrier layer effectively scatters phonons and facilitates energy exchange within different branches of phonons, preventing frequency dependence at RT. At 80 K, the Al/SiO_2/Si sample exhibited a resurgence of frequency-dependent thermal transport, resulting from the reduced interfacial phonon scattering at the interface. In addition, enhanced phonon–phonon scattering in Si at 500 K contributed to heat exchange between low- and high-energy phonons, decreasing the frequency dependence. Furthermore, our measurements on the Al/Si sample successfully extract the spectrum of phonon MFPs in Si at RT and 80 K, in agreement with first-principles calculations. Our observations emphasize the vital role of boundary conditions in frequency-dependent thermal transport, which has significant implications for the design and thermal management of high-frequency electronic devices.

II. EXPERIMENTAL DETAILS

To understand the impact of boundary conditions on the frequency-dependent thermal transport, we designed two samples with different boundary conditions. For Boundary 1, we fabricated a high-quality Al/Si interface with atomic sharpness through molecular beam epitaxy growth of Al (111) on Si (111). We used a newly grown Al/Si sample with an atomically sharp interface to avoid potential physisorption. The sample was fabricated using the same procedure as our prior work[20] with a larger thickness of the Al film. According to the diffuse mismatch model (DMM), similar Debye temperatures with matched phonon DOS provide efficient phonon transmission across the interface, leading to a low phonon scattering rate. Consequently, phonon transport across this interface is predominantly diffusive, with preserved thermal non-equilibrium between low- and high-energy phonons. For comparison, we built an interface with a much higher rate of phonon scattering to facilitate sufficient energy exchange within different branches of phonons (Boundary 2). Due to the difficulty in growing metals on Si with highly dissimilar Debye temperatures while maintaining an atomically sharp interface, we fabricated an Al/SiO_2/Si sample instead to enhance phonon scattering at the interface. Using magnetron sputtering deposition, we grew a thin Al layer on the Si substrate without moving its native oxide. The Al layer thickness in both samples was measured by picosecond acoustics, 138 nm for the Al/Si sample and 70 nm for the Al/SiO_2/Si sample, respectively.

We measured Λ of Si and G of the Al/Si interface in as-prepared samples by TDTR,[21,22] a non-contact pump-probe technique to characterize thermal transport in a variety of materials.[23–26] Briefly, we split the pulsed femtosecond laser beam (785 nm, 80 MHz repetition rate) into a pump beam and a probe beam using a polarizing beam splitter, with the relative delay time adjusted by a mechanical linear motor stage. We modulated the pump laser beam at a radio frequency f, ranging from 0.47 MHz to 10.1 MHz, through an electro-optical modulator (EOM) to induce periodic temperature oscillation on the sample surface. The probe beam monitored the corresponding temperature-dependent reflectance changes of the sample surface, modulated at an audio frequency of 200 Hz by a mechanical chopper to enhance the signal-to-noise ratio. We then demodulated the acquired signals with lock-in amplifiers. The pump and probe beams were focused to a $1/e^2$ radius of 30 μm to minimize the non-equilibrium, induced by the spot size in our measurements.[14]

We initially fitted the demodulated signals (ratio of the in-phase component and the out-of-phase component of the lock-in amplifier) with a stratified thermal model for extracting thermal properties.[21,27] The model utilized a numerical solution of the heat diffusion equation, grounded in the local-equilibrium assumption, where all energy carriers share the same temperature. This assumption implies, for instance, that there are no distinct temperature gradients between different phonon branches within the material. Accordingly, a single thermal transport channel with specified thermal parameters is sufficient for our fitting, denoted as the one-channel model, with further details provided in the supplementary material. Frequency-dependent thermal transport was only observed within the Al/Si sample at RT, while it came forth in both samples at 80 K. We then interpreted the observed frequency dependence by the two-channel model, considering non-equilibrium heat flow between low- and high-energy phonons in our TDTR measurements (see the supplementary material).

III. RESULTS AND DISCUSSION

A. Frequency-dependence at room temperature

We first conducted TDTR measurements at RT. Apparent Λ of Si and G of the Al/Si interface were extracted by the one-channel model, as depicted in Fig. 1. In the Al/Si sample with Boundary 1, Λ exhibits a pronounced frequency dependence, decreasing from 135 W m^{-1} K^{-1} at 0.47 MHz to 106 W m^{-1} K^{-1} at 10.1 MHz, which has not been observed before in Al/Si sample even with a clean interface, where native oxide is removed. We compare our results with previously reported Λ in Al/semiconductor alloys displaying frequency dependence, including $Si_{0.99}Ge_{0.01}$,[17] $Si_{0.2}Ge_{0.8}$,[18] $Si_{0.4}Ge_{0.6}$,[20] $In_{0.53}Ga_{0.47}As$,[20] and $In_{0.49}Ga_{0.51}P$.[20] We find that Λ of the Al/Si sample exhibits a comparable decreasing trend with f to that observed in $Si_{0.99}Ge_{0.01}$. Meanwhile, G increases with rising f, reaching a maximum value of 385 MW m^{-2} K^{-1} at 10.1 MHz and a minimum value of 302 MW m^{-2} K^{-1} at 0.47 MHz. The obtained maximum values of Λ and G in the Al/Si sample are in excellent agreement with literature values within the error range,[20,28] validating the accuracy of our measurements. Then, we plot representative TDTR signals with corresponding fitting curves from the one-channel model, presented in Fig. 2(a). Applying one set of parameters (Λ=135 W m^{-1} K^{-1} and G = 302 MW m^{-2} K^{-1}), the one-channel model fits well for data at 0.47 MHz but shows an obvious overestimation for data at higher frequencies, exceeding the error range. This discrepancy reveals a suppressed Λ under high-frequency periodic heating. Notably, although earlier TDTR measurements on Al/Si structures reported no discernible dependence with f at RT, the frequency dependence appears in our Al/Si sample, indicating a crucial role for the high-quality interface with atomic-level sharpness.

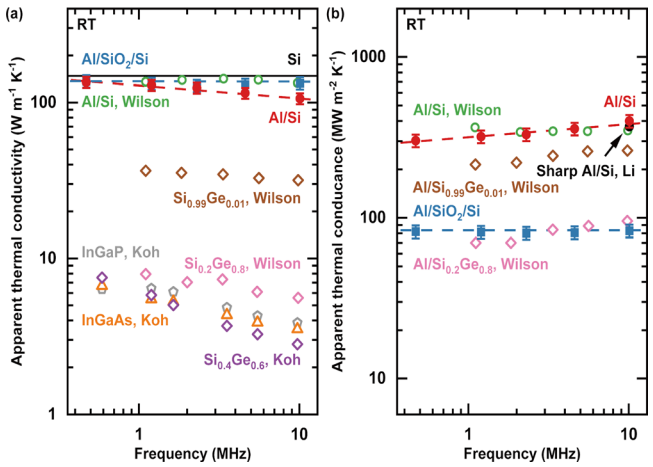

FIG. 1. Apparent (a) Λ and (b) G of Al/Si (solid red circles) and Al/SiO_2/Si (solid blue squares) samples, derived from the one-channel thermal model at RT. The solid black line represents Λ of bulk Si[28] while the solid black circle stands for G of sharp Al/Si interface by Li *et al.*[20] Open diamonds exhibit reported frequency dependence in $Si_{0.99}Ge_{0.01}$ (brown),[17] $Si_{0.2}Ge_{0.8}$ (pink),[18] and $Si_{0.4}Ge_{0.6}$ (purple).[11] Orange triangles and gray pentagons show the frequency-dependent Λ measured in $In_{0.53}Ga_{0.47}As$ and $In_{0.49}Ga_{0.51}P$, respectively.[11]

To further elucidate the impact of the boundary condition, we conducted TDTR experiments on the Al/SiO_2/Si sample with Boundary 2 at RT, where the presence of a native oxide layer between Al and Si constitutes a diffuse interface. In this sample, the measured Λ ranges from 129 W m^{-1} K^{-1} to 136 W m^{-1} K^{-1} at varying frequencies, while G varies from 80.1 MW m^{-2} K^{-1} to 82.2 MW m^{-2} K^{-1}, demonstrating no apparent frequency dependence within experimental uncertainty. Hence, a single parameter set (Λ=134 W m^{-1} K^{-1} and G) is sufficient to fit the entire frequency range of the acquired TDTR data, as shown in Fig. 2(b). The absence of frequency dependence in the Al/SiO_2/Si sample agrees with prior TDTR studies on Al/Si structures, suggesting that a diffuse thermal interface inhibits non-equilibrium heat flow in high-frequency TDTR measurements, thereby preventing the emergence of frequency dependence.[20]

As illustrated in Fig. 3, an atomically sharp interface exhibits a strong filtering effect, where the transmissivity of higher-energy phonons is remarkably lower than that of low-energy phonons. This selective transmission leads to an apparent significant temperature difference disparity between low- and high-energy phonons after passing through near the interface, establishing a state of thermal non-equilibrium.[20] This thermal non-equilibrium would give rise to an additional non-equilibrium thermal resistance, appearing as frequency dependence in pump-probe measurements.[13,17] At high pump-modulation frequencies, the temperature response is more sensitive to the thermal properties of the region near the interface, and the non-equilibrium resistance manifests as a lower apparent thermal conductivity. At low modulation frequencies, the non-equilibrium resistance contributes to a reduced thermal conductance. This is the reason for the observed frequency-dependent thermal transport in our Al/Si sample with the atomically sharp interface. In contrast, the presence of a diffuse interface would redistribute the phonon transmissivity spectra at the interface, since additional scattering centers such as atomic intermixing, roughness, oxide interlayer, and contamination would drive

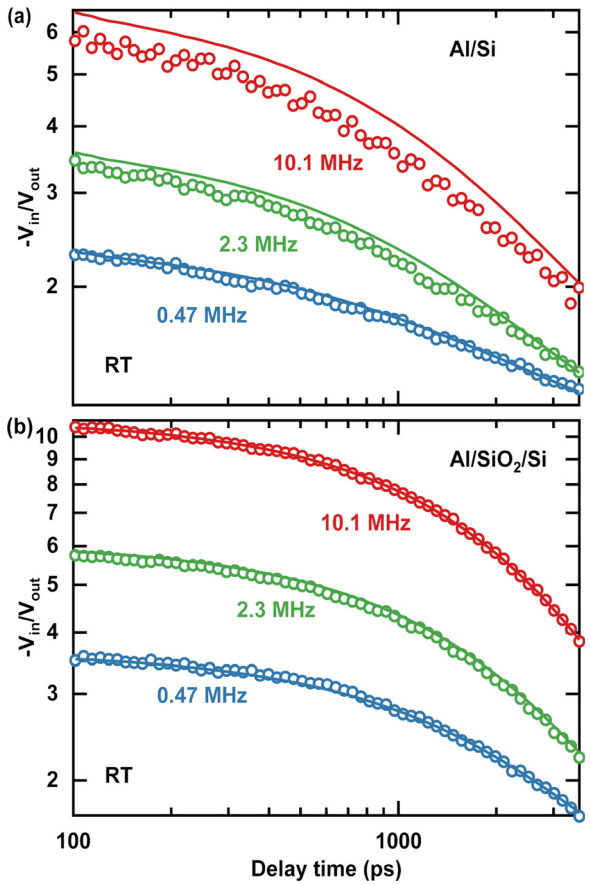

FIG. 2. Fits of the one-channel thermal model (solid lines) to TDTR signals (open circles) measured in (a) the Al/Si sample and (b) the Al/SiO_2/Si sample at various modulation frequencies. Red, green, and blue plots represent signals at frequencies of 10.1, 2.3, and 0.47 MHz, respectively. In these fits, Λ of Si is fixed at 134 W m^{-1} K^{-1} for all six curves. G is set as 302 MW m^{-2} K^{-1} for the Al/Si sample and 81 MW m^{-2} K^{-1} for the Al/SiO_2/Si sample.

energy exchange between different phonon modes. This efficiently relaxes the temperature disparity between high- and low-energy phonons, suppressing the non-equilibrium effects and eliminating the frequency dependence, as observed in our Al/SiO_2/Si sample.

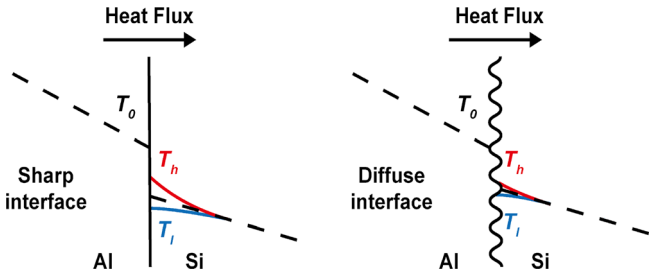

FIG. 3. Schematic illustrating temperature distributions near the sharp and diffuse interfaces. Here, T_0 represents temperature in Al near the interface. T_h and T_l are temperatures of high- and low-energy phonons in Si near the interface, respectively.

Our results necessitate a re-evaluation of existing theories regarding the absence of frequency dependence in TDTR experiments of pure Si at RT.[9,14,29,30] Previous models, including the nonlocal model by Koh *et al.*[9] and the superdiffusive model by Vermeersch *et al.*,[30] successfully explain frequency dependence in semiconductor alloys, but are insufficient to explain our results. Furthermore, they largely overlook the influence of the transducer/sample interface. In contrast, our work identifies the interface itself as a critical factor governing the frequency-dependent thermal transport, providing a more complete physical picture.

Our results support the two-channel model,[17] and underscore the critical role of transducer/sample boundary conditions in TDTR measurements. Moreover, we can contrast this perspective with the ballistic/diffusive model by Wilson *et al.*, who proposed that a low-quality interface (i.e., low thermal conductance G) increases the population of reflected low-wave vector phonons and enhances the frequency dependence.[18]

While we acknowledge that the weak coupling between transducer and long MFP phonons in the substrate would enhance thermal non-equilibrium, as confirmed in their TDTR measurements on Ta/MgO and Al/MgO samples,[18] we propose that this mechanism is primarily valid for atomically sharp interfaces that promote specular interfacial reflection of long MFP phonons. In contrast, we postulate that diffuse interfaces with additional scattering centers, such as oxide layers or imperfections, would facilitate thermal equilibration. These phonon scattering pathways between high-energy and low-energy phonons would suppress the presence of frequency dependence.

This framework can reconcile previous findings. The lack of observed frequency dependence in Al/Si at RT reported by Wilson and Cahill[18] is consistent with our hypothesis, assuming their interface was structurally diffuse—a likely condition given the challenge of removing the persistent native silicon oxide—despite exhibiting a high G that is comparable to our Al/Si sharp interface. This suggests that the value of G alone is not a sufficient predictor to dictate frequency dependence. Regarding the Al/11 nm SiO_2/Si sample exhibiting a slight decrease in Λ at 9.8 MHz,[18] we attribute this decrease to the reduced sensitivity to Λ of Si at high frequencies, an artifact caused by the significant thermal resistance of the 11 nm-thick SiO_2 layer.

Hence, we want to highlight our framework of the role of boundary conditions here. For sharp interfaces, the magnitude of frequency dependence is governed by the spectral overlap of phonons in the constituent materials, not decisively by the value of G. For diffuse interfaces, additional phonon scattering at the interface disrupts thermal non-equilibrium, thereby suppressing the frequency dependence.

B. Frequency dependence at 80 and 500 K

To validate our hypotheses of the boundary condition's role in the observed frequency dependence, we then conducted TDTR measurements on the two samples at 80 K red and 500 K and the results are exhibited in Fig. 4. At 80 K, we still observed the frequency dependence, with a relatively larger variation of 26.2 % in Λ, compared to the RT values in the Al/Si sample with Boundary 1. This is understandable since the phonon–phonon scattering is suppressed as the temperature decreases, resulting in an increased non-equilibrium thermal resistance under high heating frequencies. Importantly, despite the presence of a SiO_2 interlayer in the Al/SiO_2/Si sample, frequency dependence was observed at 80 K, with a change of 18.1 % in Λ, in

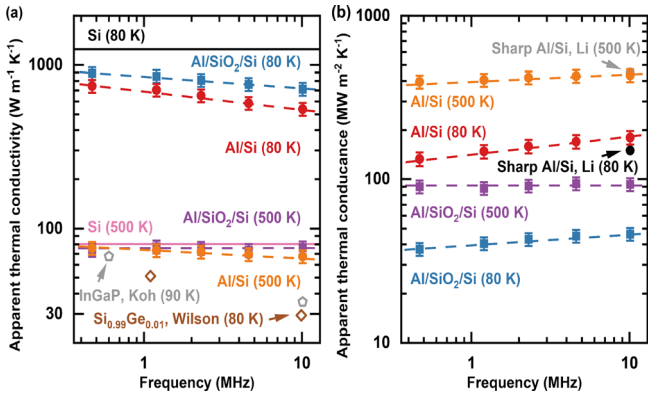

FIG. 4. Apparent (a) Λ and (b) G of Al/Si (solid circles) and Al/SiO_2/Si (solid squares) samples, derived from the one-channel thermal model at 80 K (red for Al/Si and blue for Al/SiO_2/Si) and 500 K (orange for Al/Si and purple for Al/SiO_2/Si).

sharp contrast to the room temperature behavior. The measured maximum Λ in the Al/Si sample (745 W m^{-1} K^{-1}) is lower than that in the Al/SiO_2/Si sample (890 W m^{-1} K^{-1}), while both were smaller than the reference value measured using the steady-state method. This suggests a greater non-equilibrium thermal resistance in the Al/Si sample, owing to the sharp interface. Notably, we noted that both values were smaller than those reported in bulk Si. Previous studies have pointed out that the measured in-plane thermal conductivity $\Lambda_{//}$ shows a pronounced reduction when the temperature profile length falls below the phonon MFPs, leading to spot-size dependence in TDTR measurements.[14,18] At 80 K, the longest phonon MFPs in Si reach $\sim 100\,\mu$m, exceeding the characteristic length of the temperature profile in our TDTR measurements.[14,31] However, the $1/e^2$ beam radius of 30 μm in our measurement results in a negligible sensitivity of signals to $\Lambda_{//}$ at f higher than 4 MHz (see the supplementary material). Consequently, the reduced apparent Λ at 80 K comes from non-equilibrium thermal resistance due to high-frequency heating, rather than a decreased $\Lambda_{//}$ from the finite laser spot size.

The reemerged frequency dependence in the Al/SiO_2/Si sample is attributed to two main reasons. First, phonons possess longer wavelengths and are immune to being scattered by imperfections at 80 K, thus maintaining the temperature difference between low- and high-energy phonons near the interface.[20] In consequence, the interface, even with a SiO_2 layer, is insufficient to scatter heat-carrying phonons to achieve thermal equilibrium, and the boundary condition transforms from Boundary 2 to Boundary 1 for the low-temperature case. This would result in a pronounced temperature difference between low- and high-energy phonons and observable non-equilibrium thermal resistance. Second, the interaction between phonons in silicon becomes weaker at 80 K, which helps to keep the non-equilibrium with a longer non-equilibrium distance. The extended non-equilibrium region made the frequency dependence easier to detect, and stronger phonon non-equilibrium effects facilitate the emergence of frequency dependence.[13,17] So we can observe the emergence of frequency dependence in the Al/SiO_2/Si sample at 80 K.

At 500 K, we observed the decreased frequency dependence with a smaller variation of 11.4% in Λ of the Al/Si sample with the sharp interface, ranging from 66.5 W m^{-1} K^{-1} (at 10.1 MHz) to 75.1 W m^{-1} K^{-1}

(at 0.47 MHz), while the measured Λ remains nearly constant (74.5 W m^{-1} K^{-1}) in the Al/SiO_2/Si sample. Our measurements on Λ of Si at 500 K agree well with literature values.[28] The weakened frequency dependence in the Al/Si sample can be attributed to the increased strength of phonon–phonon scattering in Si, which diminishes the profile of thermal non-equilibrium and suppresses the frequency dependence. The experimental results at 80 and 500 K confirm our proposition about the role of boundary conditions in the frequency dependence.

C. Cumulative thermal conductivity with phonon mean free path

Frequency-dependent Λ has achieved great success in probing the spectral distribution of phonon MFPs in semiconductor alloys and 2D materials Λ.[10–12] However, previous TDTR measurements on Si showed no frequency dependence, even though Si has a sufficiently broad spectrum of phonon MFPs. Although Regner *et al.* have reported a measured phonon MFPs spectrum in Si using BB-FDTR[15] from 80 K to 417 K, their thermal model has been questioned. The model has several limitations, including the neglect of weak electron–phonon coupling within the Au transducer and an oversimplified treatment of the volumetric heat source. As Wilson and Cahill[18] have discussed, these aspects are critical. Subsequently, Regner *et al.* reinterpreted their BB-FDTR results using a two-temperature model that accounted for non-surface heat deposition. This revised analysis revealed that their initially reported frequency-dependent thermal conductivity was an artifact of heat transfer within the transducer itself.[32]

Here, our study provides a more accurate approximation of the phonon MFP distribution in silicon at room temperature and 80 K, where we consider that ballistic phonons with characteristic lengths larger than $2d = 2\sqrt{\Lambda/\pi Cf}$ do not contribute to the measured thermal conductivity, where C is the volumetric heat capacity. Although Koh and Cahill initially proposed to employ $L = d$ as the characteristic length to probe the accumulation function of phonon MFPs,[10] da Cruz *et al.* later suggested that the reduction in the measured thermal conductivity could instead be due to insensitivity of TDTR measurements to phonons with $L_{anh} > 3d$, where LL_{anh} is the MFP of phonons with considering anharmonic scattering.[33] However, our previous Boltzmann transport equation calculations have pointed out that as long as the distribution of phonon MFPs is sufficiently wide, the apparent thermal conductivity measured by TDTR can be crudely approximated by ballistic phonons with a characteristic length of $2d$, which do not contribute to the measured thermal response in pump-probe experiments.[9,10] This is validated in our earlier measurements of black phosphorus[12] and graphite.[11] Therefore, we choose $L = 2d$ here as the corresponding phonon MFP in the TDTR measurements. The results are illustrated in Fig. 5.

For the Al/Si sample, our data exhibit remarkable agreement with the first-principles calculation by Jiang *et al.*[19] at RT. The agreement between our measurements and first-principles calculations indicates that the selection of $L = 2d$ is appropriate. At 80 K, our measurements align closely with first-principles results, calculated through interpolation of calculations by Minnich *et al.* at 100 and 60 K,[14] with a slight deviation for phonons with short MFPs. This deviation is attributed to the mismatched phonon DOS between Al and Si, particularly for high-frequency phonons (higher than 10 THz) in Si, which are either reflected or decomposed to low-energy phonons at the interface. As a result, we cannot accurately probe their contribution to the cumulative

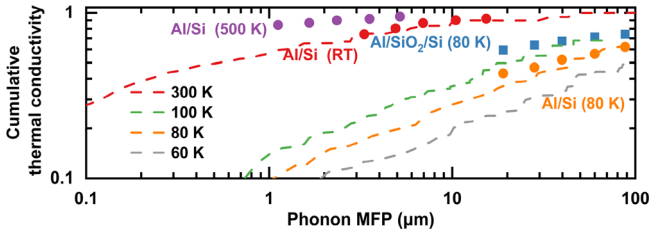

FIG. 5. Phonon MFP spectra for Si at RT and 80 K. Dashed lines represent first-principles calculations of bulk Si at 300 K (red) by Jiang *et al.*,[19] 100 K (green), and 60 K (gray) by Minnich *et al.*[14] The dashed orange line denotes the cumulative Λ at 80 K, calculated from interpolating values between 100 and 60 K by Minnich *et al.* Solid circles exhibit our measurements in the Al/Si sample at 500 K (purple), RT (red), and 80 K (orange), while solid blue squares display measurements on the Al/SiO_2/Si sample.

Λ. At 500 K, we observed the phonon MFP spectrum shift from that at 300 K, which comes from increased phonon–phonon scattering and saturated heat capacity. For the Al/SiO_2/Si sample, the calculated cumulative Λ with phonon MFP displays large deviations from the first-principles calculation. The difference can be explained by the diffuse interface, which effectively reduces the ballistic phonon population, thereby limiting the extraction of intrinsic spectral phonon MFPs.

This discovery emphasizes the feasibility of frequency dependence to accurately measure spectral phonon MFPs, depending on the proper selection of boundary conditions. To accurately probe the spectral phonon MFPs, a boundary condition with minimal phonon scattering at the transducer/sample interface is crucial. Specifically, not only an atomically sharp interface but also a metal transducer with a matched or larger Debye temperature is required. For example, we postulate that Al is a better transducer material, compared to Ta, to measure the spectral phonon MFPs of Si. There are two reasons. First, Ta shows a more dissimilar Debye temperature to Si, leaving a higher interfacial phonon scattering rate, especially for high-energy phonons. Second, Ta has a higher density of states for low-energy phonons, leading to a smaller temperature difference between low- and high-energy phonons in Si, compared to the Al transducer. On the contrary, if we want a TDTR measurement without any frequency dependence, a metal transducer with a low Debye temperature and a diffuse interface is preferred.

D. Two-channel model for non-equilibrium thermal transport

To quantitatively analyze the observed frequency dependence, we also applied the two-channel model to fit TDTR data (see the supplementary material). In the model, we divide the low-energy phonons (< 3 THz, Channel 1) and high-energy phonons (> 3 THz, Channel 2) into separate channels, where there is a coupling factor g between the two channels. We select the partition frequency (3 THz) based on the principle that only phonon modes with linear dispersion and low heat capacity are considered in the low-frequency Channel 1.[34] The heat capacities of Channel 1 (C_1) and Channel 2 (C_2) are derived from calculations of the phonon density of states in Si,[34] and at RT, we obtained $C_1 = 3 \times 10^4$ J m^{-3} K^{-1} and $C_2 = 1.62 \times 10^6$ J m^{-3} K^{-1}. At 80 and 500 K, we assumed that C_1 remained relatively unchanged

compared to the value at RT, and C_2 increased with increasing temperature since the majority of high-energy phonons would be thermalized only at higher temperatures. Acquired TDTR signals can be well fit for the entire frequency range, using a set of thermal conductivity contributed by Channel 1 (Λ_1) and Channel 2 (Λ_2), interfacial thermal conductance from Channel 1 (G_1) and Channel 2 (G_2), and g. We show the acquired total Λ and G in Fig. 6, with a comparison of previous calculations and experimental data. In the Al/Si sample, we obtained $\Lambda_1 = 66\,\mathrm{W\,m^{-1}\,K^{-1}}$, $\Lambda_2 = 75\,\mathrm{W\,m^{-1}\,K^{-1}}$, $G_1 = 58\,\mathrm{MW\,m^{-2}\,K^{-1}}$, $G_2 = 400\,\mathrm{MW\,m^{-2}\,K^{-1}}$, and $g = 1.2 \times 10^{14}\,\mathrm{W\,m^{-3}\,K^{-1}}$ at RT. The total thermal conductivity $\Lambda_1 + \Lambda_2 = 141\,\mathrm{W\,m^{-1}\,K^{-1}}$ aligns well with previously reported values.[18,28,35] Low-frequency phonons in Channel 1 contribute 46.8 % of the total Λ while high-frequency phonons contribute 53.2 %, which is consistent with theoretical predictions.[36] The obtained coupling factor g lies on the order of $10^{14}\,\mathrm{W\,m^{-3}\,K^{-1}}$, which is expected by the scattering rates of low-frequency phonons.[37,38] The total thermal conductance $G_1 + G_2 = 458\,\mathrm{MW\,m^{-2}\,K^{-1}}$ matched the value predicted by the DMM.[20] We attribute the apparent agreement between our measurements and DMM results to the combined influence of inelastic phonon transport and electron–phonon coupling. The DMM underestimates the phonon–phonon thermal conductance of the metal/nonmetal interface since it neglects the contribution by inelastic phonon transport. However, this underestimation is offset by electron–phonon coupling within the metal layer, which reduces the measured thermal conductance.[39] Hence, the underestimation by the DMM is fortuitously compensated by the reduction from electron–phonon coupling within Al, resulting in a good, albeit coincidental, agreement with our measurements. The result suggests the presence of inelastic phonon transport in the Al/Si interface even at RT.

Furthermore, we also fit the TDTR data acquired in the Al/Si sample at 500 K by the two-channel model and got the values of $\Lambda_1 = 32\,\mathrm{W\,m^{-1}\,K^{-1}}$, $\Lambda_2 = 44.5\,\mathrm{W\,m^{-1}\,K^{-1}}$, $G_1 = 80\,\mathrm{MW\,m^{-2}\,K^{-1}}$, $G_2 = 405\,\mathrm{MW\,m^{-2}\,K^{-1}}$, and $g = 4 \times 10^{14}\,\mathrm{W\,m^{-3}\,K^{-1}}$. The measured total thermal conductivity $\Lambda_1 + \Lambda_2 = 76.5\,\mathrm{W\,m^{-1}\,K^{-1}}$ is in good agreement with literature values.[18,28,35] The relatively larger coupling factor g at 500 K arises from increased phonon–phonon scattering rate. Importantly, we observed a relatively smaller difference (fivefold) between the thermal conductance G of the two channels at 500 K, compared to that at RT (eightfold). This originates from the enhanced phonon–phonon coupling at 500 K, and explains the weakened frequency dependence at 500 K.

In addition, we obtained $\Lambda_1 = 630\,\mathrm{W\,m^{-1}\,K^{-1}}$, $\Lambda_2 = 320\,\mathrm{W\,m^{-1}\,K^{-1}}$, $G_1 = 22\,\mathrm{MW\,m^{-2}\,K^{-1}}$, $G_2 = 162\,\mathrm{MW\,m^{-2}\,K^{-1}}$, and $g = 2 \times 10^{12}\,\mathrm{W\,m^{-3}\,K^{-1}}$ in the Al/Si sample with the sharp interface at 80 K. The total Λ of $950\,\mathrm{W\,m^{-1}\,K^{-1}}$ is still lower than previously reported values in Si, which probably arises from the suppressed $\Lambda_{//}$ due to a not large enough laser spot size. The partial Λ contributed by Channel 1 increases to 66.5 %, which is consistent with the expectation that low-energy phonons play a more significant part in Λ at lower temperatures. Besides, the total $G = 184\,\mathrm{MW\,m^{-2}\,K^{-1}}$ confirms DMM predictions within the measurement uncertainty. Moreover, the coupling factor g diminishes to the order of $10^{12}\,\mathrm{W\,m^{-3}\,K^{-1}}$, originating from the reduced phonon–phonon scattering rates at 80 K. Meanwhile, we also applied the two-channel model to analyze TDTR data of the Al/SiO_2/Si sample at 80 K. The obtained thermal conductivities for the two channels, $\Lambda_1 = 640\,\mathrm{W\,m^{-1}\,K^{-1}}$ and $\Lambda_2 = 360\,\mathrm{W\,m^{-1}\,K^{-1}}$, correspond to the values of the Al/Si sample. Moreover, the coupling factor is $g = 4 \times 10^{12}\,\mathrm{W\,m^{-3}\,K^{-1}}$, which is also on the order of that in the Al/Si sample. In contrast, we obtained $G_1 = 11.5\,\mathrm{MW\,m^{-2}\,K^{-1}}$ and $G_2 = 32.5\,\mathrm{MW\,m^{-2}\,K^{-1}}$, which show a much smaller difference (threefold) compared to that of the Al/Si sample (eightfold). This means that the temperature difference at the surface in the Al/Si sample is remarkably larger than that in the Al/SiO_2/Si sample, which explains why the frequency dependence is more significant in the Al/Si sample. Our analysis using the two-channel model further validates our assumptions about the role of transducer/sample boundary conditions in the frequency dependence in pump-probe experiments.

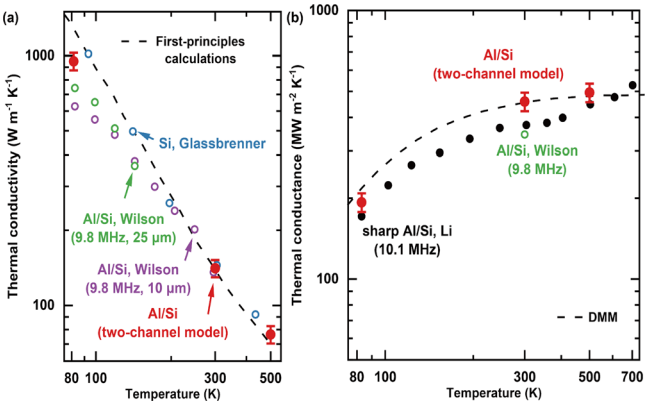

FIG. 6. Total (a) Λ and (b) G of the Al/Si sample, extracted by the two-channel model (solid red circles). The dashed black lines represent predicted Λ from first-principles calculations[35] in (a) and G by DMM[20] in (b). Open circles in (a) denote Λ of Si measured by Glassbrenner *et al.* using steady-state techniques (blue)[28] and by Wilson *et al.* using TDTR, with a modulation frequency of 9.8 MHz and spot sizes of 25 μm (green) and 10 μm (purple).[18] Circles in (b) display G of Al/Si interface measured by Wilson *et al.* (9.8 MHz, green)[18] and Li *et al.* (10.1 MHz, black)[20] using TDTR.

IV. SUMMARY

In summary, our TDTR measurements observed the frequency-dependent thermal transport in Si with an atomically sharp Al/Si interface at RT. The dependence is previously buried due to the lack of high-quality sharp interfaces, as validated by measurements on the Al/SiO_2/Si sample. In this context, imperfections at the interface would facilitate energy exchange between different phonon branches and prohibit the non-equilibrium effects. In addition, the governance of the diffuse interface is restricted at cryogenic temperatures, where phonons with longer MFPs exhibiting lower interfacial scattering rates would enhance the non-equilibrium heat flow. Moreover, increased phonon–phonon scattering in Si at higher temperatures helps facilitate energy exchange between low- and high-energy phonons and suppress the frequency dependence. Our findings offer a deeper comprehension of frequency dependence in TDTR experiments, expanding the purview of non-Fourier thermal transport. We propose that frequency dependence is a common phenomenon in TDTR experiments mediated by boundary conditions, rather than a material-specific anomaly, which is vital for accurately measuring thermal properties through TDTR. Furthermore, this work holds great importance for future heat dissipation strategies of high-frequency electronics.

SUPPLEMENTARY MATERIAL

See the supplementary material for detailed information on the one-channel model and the two-channel model for fitting TDTR measurements with sensitivity and uncertainty analysis.

ACKNOWLEDGMENTS

We acknowledge receiving funding support from the National Natural Science Foundation of China (Grant Nos. 52161145502 and 12004211), the Shenzhen Science and Technology Program (Grant Nos. RCYX20200714114643187 and WDZC20200821100123001), the Tsinghua Shenzhen International Graduate School (Grant Nos. QD2021008N and JC2021008), and the Guangdong Special Support Program (Grant No. 2023TQ07A273).

AUTHOR DECLARATIONS

Conflict of Interest

The authors have no conflicts to disclose.

Author Contributions

Yizhe Liu: Conceptualization (equal); Data curation (equal); Formal analysis (equal); Investigation (equal); Methodology (equal); Software (equal); Writing – original draft (equal). **Qinshu Li:** Data curation (supporting). **Fang Liu:** Resources (supporting). **Xinqiang Wang:** Supervision (supporting). **Bo Sun:** Conceptualization (equal); Funding acquisition (equal); Supervision (equal); Validation (equal); Writing – review & editing (equal).

DATA AVAILABILITY

The data that support the findings of this study are available from the corresponding author upon reasonable request.

The solid lines represent Λ of bulk Si at 80 K (black) and 500 K (pink)[28] while the solid circles stand for G of sharp Al/Si interface by Li *et al.* at 80 K (black) and 500 K (gray).[20] Open brown diamonds exhibit reported frequency dependence in $Si_{0.99}Ge_{0.01}$,[18] and gray pentagons show the frequency-dependent Λ measured in $In_{0.49}Ga_{0.51}P$ at 90 K.[10]

REFERENCES

[1]G. Chen, Nat. Rev. Phys. **3**, 555 (2021).
[2]G. Mahan and F. Claro, Phys. Rev. B **38**, 1963 (1988).
[3]M. G. Kanatzidis, Chem. Mater. **22**, 648 (2010).
[4]E. Pop, Nano Res. **3**, 147 (2010).
[5]P. Sverdrup, S. Sinha, M. Asheghi, S. Uma, and K. Goodson, Appl. Phys. Lett. **78**, 3331 (2001).
[6]H. Y. Chiu, V. V. Deshpande, H. W. C. Postma, C. N. Lau, C. Miko, L. Forro, and M. Bockrath, Phys. Rev. Lett. **95**, 226101 (2005).
[7]G. Chen, Phys. Rev. B **57**, 14958 (1998).
[8]G. Chen, Phys. Rev. Lett. **86**, 2297 (2001).
[9]Y. K. Koh, D. G. Cahill, and B. Sun, Phys. Rev. B **90**, 205412 (2014).
[10]Y. K. Koh and D. G. Cahill, Phys. Rev. B **76**, 075207 (2007).
[11]B. Sun, L. Zhao, Z. Chen, S. Hu, A. Zhi, J. Wu, F. Kang, X. Tian, and X. Gu, PREPRINT (Version 1) Research Square:10.21203/rs.3.rs-5186005/v1 (2024).
[12]B. Sun, X. Gu, Q. Zeng, X. Huang, Y. Yan, Z. Liu, R. Yang, and Y. K. Koh, Adv. Mater. **29**, 1603297 (2017).
[13]P. Jiang, X. Qian, X. Gu, and R. Yang, Adv. Mater. **29**, 1701068 (2017).
[14]A. J. Minnich, J. A. Johnson, A. J. Schmidt, K. Esfarjani, M. S. Dresselhaus, K. A. Nelson, and G. Chen, Phys. Rev. Lett. **107**, 095901 (2011).
[15]K. T. Regner, D. P. Sellan, Z. Su, C. H. Amon, A. J. McGaughey, and J. A. Malen, Nat. Commun. **4**, 1640 (2013).
[16]J. P. Freedman, J. H. Leach, E. A. Preble, Z. Sitar, R. F. Davis, and J. A. Malen, Sci. Rep **3**, 2963 (2013).
[17]R. Wilson, J. P. Feser, G. T. Hohensee, and D. G. Cahill, Phys. Rev. B **88**, 144305 (2013).
[18]R. Wilson and D. G. Cahill, Nat. Commun. **5**, 5075 (2014).
[19]P. Jiang, L. Lindsay, and Y. K. Koh, J. Appl. Phys. **119**, 245705 (2016).
[20]Q. Li, F. Liu, S. Hu, H. Song, S. Yang, H. Jiang, T. Wang, Y. K. Koh, C. Zhao, F. Kang *et al.*, Nat. Commun. **13**, 4901 (2022).
[21]D. G. Cahill, Rev. Sci. Instrum. **75**, 5119 (2004).
[22]B. Sun and Y. K. Koh, Rev. Sci. Instrum. **87**, 064901 (2016).
[23]B. Sun, S. Niu, R. P. Hermann, J. Moon, N. Shulumba, K. Page, B. Zhao, A. S. Thind, K. Mahalingam, J. Milam-Guerrero *et al.*, Nat. Commun. **11**, 6039 (2020).
[24]Y. Liu, Q. Li, Y. Qian, Y. Yang, S. Wang, W. Li, and B. Sun, Appl. Phys. Lett. **122**, 222201 (2023).
[25]Y. Wang, R. Luo, J. Chen, X. Zhou, S. Wang, J. Wu, F. Kang, K. Yu, and B. Sun, Phys. Rev. Lett. **132**, 264101 (2024).
[26]Y. Liu, X. Zhou, S. Wang, and B. Sun, Mod. Phys. Lett. B **39**, 2550052 (2025).
[27]A. Feldman, High Temp.-High Press. **31**, 293 (1999).
[28]C. J. Glassbrenner and G. A. Slack, Phys. Rev. **134**, A1058 (1964).
[29]D. Ding, X. Chen, and A. J. Minnich, Appl. Phys. Lett. **104**, 143104 (2014).
[30]B. Vermeersch, J. Carrete, N. Mingo, and A. Shakouri, Phys. Rev. B **91**, 085202 (2015).
[31]R. Gereth and K. Hubner, Phys. Rev. **134**, A235 (1964).
[32]K. T. Regner, L. C. Wei, and J. A. Malen, J. Appl. Phys. **118**, 235101 (2015).
[33]C. A. da Cruz, W. Li, N. A. Katcho, and N. Mingo, Appl. Phys. Lett. **101**, 083108 (2012).
[34]A. Zdetsis and C. Wang, Phys. Rev. B **19**, 2999 (1979).
[35]M. Asheghi, K. Kurabayashi, R. Kasnavi, and K. Goodson, J. Appl. Phys. **91**, 5079 (2002).
[36]X. Wang and B. Huang, Sci. Rep. **4**, 6399 (2014).
[37]A. Ward and D. Broido, Phys. Rev. B **81**, 085205 (2010).
[38]A. A. Maznev, J. A. Johnson, and K. A. Nelson, Phys. Rev. B **84**, 195206 (2011).
[39]A. Majumdar and P. Reddy, Appl. Phys. Lett. **84**, 4768 (2004).